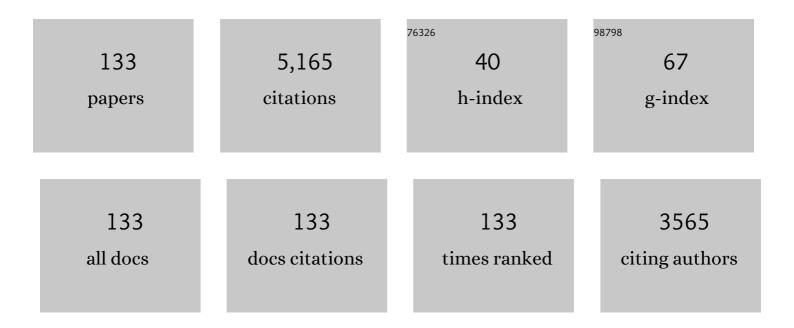
List of Publications by Year in descending order

Source: https://exaly.com/author-pdf/3644562/publications.pdf Version: 2024-02-01



#	Article	IF	CITATIONS
1	Pearlite formation via martensite. Composites Part B: Engineering, 2022, 238, 109859.	12.0	7
2	Formation of Î,-Fe ₃ C Cementite via Î,′-Fe ₃ C (ω-Fe ₃ C) in Fe–C Alloys. Crystal Growth and Design, 2021, 21, 1683-1688.	3.0	4
3	{332}<113> Twinning transfer behavior and its effect on the twin shape in a beta-type Ti-23.1Nb-2.0Zr-1.0O alloy. Journal of Materials Science and Technology, 2021, 91, 58-66.	10.7	11
4	A transition of ω-Fe3C → ω′-Fe3C → θ′-Fe3C in Fe-C martensite. Scientific Reports, 20	0303, 10, 6	081.
5	Metastable ï‰â€²-Fe3C carbide formed during ï‰-Fe3C particle coarsening in binary Fe-C alloys. Journal of Applied Physics, 2019, 125, 175112.	2.5	3
6	Twinning behavior of orthorhombic-α―martensite in a Ti-7.5Mo alloy. Science and Technology of Advanced Materials, 2019, 20, 401-411.	6.1	39
7	Simulated electron diffraction patterns of ω-Fe in Fe-C martensite. Journal of Applied Physics, 2019, 125, .	2.5	9
8	TEM investigations on lath martensite substructure in quenched Fe-0.2C alloys. Materials Characterization, 2018, 135, 175-182.	4.4	33
9	Enhanced high-temperature strength of HfB2–SiC composite up to 1600°C. Journal of the European Ceramic Society, 2018, 38, 1152-1157.	5.7	18
10	ω-Fe particle size and distribution in high-nitrogen martensitic steels. Journal of Materials Science, 2018, 53, 5339-5355.	3.7	23
11	Electron diffraction analysis of quenched Fe–C martensite. Journal of Materials Science, 2018, 53, 2976-2984.	3.7	28
12	A Simple Method for Observing <i>ï‰</i> -Fe Electron Diffraction Spots from <112> _{<i>î±</i>-Fe} Directions of Quenched Fe–C Twinned Martensite. ISIJ International, 2018, 58, 159-164.	1.4	22
13	Microstructure of ultrahigh carbon martensite. Progress in Natural Science: Materials International, 2018, 28, 749-753.	4.4	14
14	Lath formation mechanisms and twinning as lath martensite substructures in an ultra low-carbon iron alloy. Scientific Reports, 2018, 8, 14264.	3.3	34
15	In situ heating TEM observations on carbide formation and α-Fe recrystallization in twinned martensite. Scientific Reports, 2018, 8, 14454.	3.3	21
16	Deformation-induced nontetragonality of martensite in carbon steels. Materials Letters, 2018, 227, 213-216.	2.6	6
17	An atomic mechanism for the formation of nanotwins in high carbon martensite. Journal of Alloys and Compounds, 2018, 767, 68-72.	5.5	18
18	Nanoclusters of α-Fe naturally formed in twinned martensite after martensitic transformation. Journal of Applied Physics, 2018, 123, .	2.5	12

#	Article	IF	CITATIONS
19	Cubic martensite in high carbon steel. Physical Review Materials, 2018, 2, .	2.4	4
20	Impact of ruthenium on mechanical properties, biological response and thermal processing of β-type Ti–Nb–Ru alloys. Acta Biomaterialia, 2017, 48, 461-467.	8.3	17
21	Extraordinary high strength Ti-Zr-Ta alloys through nanoscaled, dual-cubic spinodal reinforcement. Acta Biomaterialia, 2017, 53, 549-558.	8.3	50
22	Microstructural Evolution and Carbides in Quenched Ultra-low Carbon (Fe–C) Alloys. ISIJ International, 2017, 57, 1233-1240.	1.4	32
23	Twinning Boundary ω-Fe Makes Carbon Martensite Hard In Steels. , 2017, , .		0
24	Novel Ti-Ta-Hf-Zr alloys with promising mechanical properties for prospective stent applications. Scientific Reports, 2016, 6, 37901.	3.3	46
25	Investigations into Ti–(Nb,Ta)–Fe alloys for biomedical applications. Acta Biomaterialia, 2016, 32, 336-347.	8.3	61
26	Anomalous phase stability of surface and interior in a metastable Ti-Nb-Zr alloy. Materials Letters, 2016, 169, 210-213.	2.6	9
27	Twin structure of the lath martensite in low carbon steel. Progress in Natural Science: Materials International, 2016, 26, 169-172.	4.4	70
28	A new nanoscale metastable iron phase in carbon steels. Scientific Reports, 2015, 5, 15331.	3.3	34
29	Understanding Solid–Solid (fccÂ→Âï‰Â+Âbcc) Transition at Atomic Scale. Acta Metallurgica Sinica (English) T	j ETQq1 1	0784314 31
30	B22-O-04The discovery of ω-Fe in common steels by TEM and XRD. Microscopy (Oxford, England), 2015, 64, i48.2-i48.	1.5	0
31	Effect of Pd addition on the microstructure of Ti-30Nb alloy. Metals and Materials International, 2015, 21, 617-622.	3.4	8
32	Enhanced yielding strength of near-α Ti–Al–Zr–Sn high temperature alloys. Materials Science & Engineering A: Structural Materials: Properties, Microstructure and Processing, 2015, 625, 131-139.	5.6	9
33	Review on ω Phase in Body-Centered Cubic Metals and Alloys. Acta Metallurgica Sinica (English Letters), 2014, 27, 1-11.	2.9	91
34	Suppression effect of oxygen on the <i>β</i> to <i>ω</i> transformation in a <i>β</i> -type Ti alloy: insights from first-principles. Modelling and Simulation in Materials Science and Engineering, 2014, 22, 015007.	2.0	22
35	{112}ã€^111〉 Twinning during ω to body-centered cubic transition. Acta Materialia, 2014, 62, 122-128.	7.9	74
36	Effect of Zr and Si addition on high temperature mechanical properties of near-α Ti–Al–Zr–Sn based alloys. Materials Science & Engineering A: Structural Materials: Properties, Microstructure and Processing, 2014, 612, 456-461.	5.6	37

#	Article	IF	CITATIONS
37	Controlled Photocatalytic Growth of Ag Nanocrystals on Brookite and Rutile and Their SERS Performance. ACS Applied Materials & Interfaces, 2014, 6, 236-243.	8.0	14
38	Microstructure and oxidation behaviors of near-α Ti-6.5Al-4Sn-4Zr-0.5Mo-based alloys with Ir addition. Journal of Materials Science, 2013, 48, 3363-3369.	3.7	6
39	Structure characterization and photoluminescence properties of (Y0.95â^²xGdxEu0.05)2O3 red phosphors converted from layered rare-earth hydroxide (LRH) nanoflake precursors. Journal of Alloys and Compounds, 2013, 559, 188-195.	5.5	36
40	Microstructure and oxidation behavior of Ti–6Al–2Zr–1Mo–1V-based alloys with Sc addition. Materials Science & Engineering A: Structural Materials: Properties, Microstructure and Processing, 2013, 580, 266-272.	5.6	13
41	Atom probe analysis on interaction between Cr and N in bake-hardening steels with anti-aging properties at RT. Materials Science & Engineering A: Structural Materials: Properties, Microstructure and Processing, 2013, 585, 100-107.	5.6	3
42	Microstructural characterization on martensitic α″ phase in Ti–Nb–Pd alloys. Journal of Alloys and Compounds, 2013, 577, S423-S426.	5.5	12
43	A popular metastable omega phase in body-centered cubic steels. Materials Chemistry and Physics, 2013, 139, 830-835.	4.0	50
44	THE ω PHASE IN A LOW ALLOY MARTENSITIC STEEL. Jinshu Xuebao/Acta Metallurgica Sinica, 2013, 49, 769.	0.3	7
45	Scandium (Sc) Behavior in High Temperature Ti Alloys. Key Engineering Materials, 2012, 520, 57-62.	0.4	0
46	Metal-Doped Magnetite Thin Films. Journal of Nanoscience and Nanotechnology, 2012, 12, 5087-5090.	0.9	2
47	Effects of Sc addition on the microstructure and tensile properties of Ti–6.6Al–5.5Sn–1.8Zr alloy. Materials Chemistry and Physics, 2012, 136, 1015-1021.	4.0	19
48	Formation of Perpendicular Graphene Nanosheets on LiFePO ₄ : A First-Principles Characterization. Journal of Physical Chemistry C, 2012, 116, 17650-17656.	3.1	28
49	Interstitial-interstitial interaction of oxygen atoms in a Nb-based ternary body-centered-cubic system. Journal of Applied Physics, 2011, 109, 113536.	2.5	1
50	Formation of the reversed austenite during intercritical tempering in a Fe–13%Cr–4%Ni–Mo martensitic stainless steel. Materials Letters, 2010, 64, 1411-1414.	2.6	100
51	Microstructural evolution and low temperature impact toughness of a Fe–13%Cr–4%Ni–Mo martensitic stainless steel. Materials Science & Engineering A: Structural Materials: Properties, Microstructure and Processing, 2010, 527, 614-618.	5.6	119
52	Microstructure Investigation on the Triple Junction with an Adjoining Twin Boundary in Nanocrystalline Palladium. Journal of Materials Science and Technology, 2010, 26, 1047-1050.	10.7	7
53	Modeling and control of the high damping behavior in Ti–Nb–O alloys. Materials Science & Engineering A: Structural Materials: Properties, Microstructure and Processing, 2009, 521-522, 372-375.	5.6	16
54	Microstructural evolution and ductility improvement of a Ti–30Nb alloy with Pd addition. Journal of Alloys and Compounds, 2009, 471, 248-252.	5.5	43

#	Article	IF	CITATIONS
55	Determination of grain size by XRD profile analysis and TEM counting in nano-structured Cu. Journal of Alloys and Compounds, 2009, 476, 113-117.	5.5	76
56	The evolution of Î∙ phase in Ni–Co base superalloys. Materials Science & Engineering A: Structural Materials: Properties, Microstructure and Processing, 2008, 485, 651-656.	5.6	48
57	Phase constituents in Ni–Al–Co–Ti quaternary alloys. Intermetallics, 2008, 16, 910-916.	3.9	26
58	Anisotropy of Snoek relaxation in a highly textured Ti–Nb–O β-Ti alloy. Journal of Applied Physics, 2008, 104, .	2.5	2
59	Single dominant distribution of Ge nanogranule embedded in Al oxide thin film. Journal of Applied Physics, 2008, 104, 104305.	2.5	4
60	Stress-induced α″ martensitic (110) twinning in β-Ti alloys. Applied Physics Letters, 2008, 93, .	3.3	45
61	Phase Constituents and Compressive Yield Stress of Ni-Co Base Alloys. Materials Transactions, 2008, 49, 424-427.	1.2	13
62	Natural mechanism of the broadened Snoek relaxation profile in ternary body-centered-cubic alloys. Physical Review B, 2007, 75, .	3.2	19
63	Atom Probe Investigation of Ruthenium Distributions around Rhenium, Molybdenum and Tungsten in a Gamma Phase of 5th-Generation Nickel-Base Single-Crystal Superalloys. Materials Transactions, 2007, 48, 566-569.	1.2	7
64	Stability of nanoscale co-precipitates in a superalloy: A combined first-principles and atom probe tomography study. Physical Review B, 2007, 76, .	3.2	38
65	Microstructure of a newly developed γ′ strengthened Co-base superalloy. Ultramicroscopy, 2007, 107, 791-795.	1.9	32
66	Grain boundary segregation in a Ni–Fe-based (Alloy 718) superalloy. Materials Science & Engineering A: Structural Materials: Properties, Microstructure and Processing, 2007, 456, 99-102.	5.6	84
67	Design and property control of Ti–M–O high damping alloys. Physica Scripta, 2007, T129, 261-264.	2.5	1
68	A New Co-Base Superalloy Strengthened by γ′ Phase. Materials Transactions, 2006, 47, 2099-2102.	1.2	35
69	Atom Probe Microanalysis of Fifth-Generation Ni-Base Single-Crystal Superalloys. Nippon Kinzoku Gakkaishi/Journal of the Japan Institute of Metals, 2006, 70, 184-187.	0.4	0
70	Effects of Ru additions on the microstructure and phase stability of Ni-base superalloy, UDIMET 720LI. Metallurgical and Materials Transactions A: Physical Metallurgy and Materials Science, 2006, 37, 355-360.	2.2	22
71	Phase stability and yield stress of Ni-base superalloys containing high Co and Ti. Metallurgical and Materials Transactions A: Physical Metallurgy and Materials Science, 2006, 37, 3183-3190.	2.2	49
72	TEM investigations on martensite in a Ti–Nb-based shape memory alloy. Scripta Materialia, 2006, 54, 1305-1310.	5.2	73

#	Article	IF	CITATIONS
73	Magnetic properties and microstructure of Fe3B/Pr2Fe14B-type nanocomposite magnets with Co and Cr additions. Journal of Magnetism and Magnetic Materials, 2006, 299, 136-144.	2.3	17
74	Snoek-Type High-Damping Alloys Realized in β-Ti Alloys with High Oxygen Solid Solution. Advanced Materials, 2006, 18, 1541-1544.	21.0	57
75	Microstructural evolution in 13Cr–8Ni–2.5Mo–2Al martensitic precipitation-hardened stainless steel. Materials Science & Engineering A: Structural Materials: Properties, Microstructure and Processing, 2005, 394, 285-295.	5.6	164
76	Investigation on structure-magnetic property correlation in melt-spun Sm(Co0.56Fe0.31Cu0.04Zr0.05B0.04)z ribbons. Journal of Magnetism and Magnetic Materials, 2005, 292, 150-158.	2.3	10
77	Microstructure and shape memory behavior of a Ti?30Nb?3Pd alloy. Scripta Materialia, 2005, 52, 1287-1291.	5.2	94
78	Microstructure and magnetic properties of melt-spun Sm(Co0.58Fe0.31Cu0.04Zr0.05B0.02)z ribbons. Journal of Applied Physics, 2004, 95, 4962-4967.	2.5	23
79	Microstructural evolution and the magnetic properties of melt-spun Sm–Co–Cu–B and Sm–Co–Fe–Cu–B ribbons. Journal of Magnetism and Magnetic Materials, 2004, 284, 321-329.	2.3	12
80	Microstructural characterization of α-Fe/Sm–Fe–N nanocomposite hard magnets. Journal of Magnetism and Magnetic Materials, 2004, 277, 337-343.	2.3	9
81	Low cycle fatigue behavior of nickel-based superalloy GH4145/SQ at elevated temperature. Materials Science & Engineering A: Structural Materials: Properties, Microstructure and Processing, 2004, 373, 54-64.	5.6	38
82	In situ formed two-phase metallic glass with surface fractal microstructure. Acta Materialia, 2004, 52, 2441-2448.	7.9	239
83	The effect of Cu on mechanical and precipitation properties of Al–Zn–Mg alloys. Journal of Alloys and Compounds, 2004, 378, 52-60.	5.5	124
84	Atom probe characterization of plate-like precipitates in a Mg–RE–Zn–Zr casting alloy. Scripta Materialia, 2003, 48, 1017-1022.	5.2	144
85	Enhanced magnetic properties of Nd–Fe–B thin films crystallized by heat treatment. Journal of Magnetism and Magnetic Materials, 2003, 260, 406-414.	2.3	19
86	Microstructure of soft magnetic FeCo–O(–Zr) films with high saturation magnetization. Journal of Magnetism and Magnetic Materials, 2003, 265, 83-93.	2.3	11
87	Microstructural control of Nb addition in nanocrystalline hard magnets with different Nd content. IEEE Transactions on Magnetics, 2003, 39, 2935-2937.	2.1	17
88	FeCo–Zr–O nanogranular soft-magnetic thin films with a high magnetic flux density. Applied Physics Letters, 2003, 82, 946-948.	3.3	74
89	Optimization of the microstructure and properties of Co-substituted Fe–Si–B–Nb–Cu nanocrystalline soft magnetic alloys. Journal of Applied Physics, 2003, 93, 9186-9194.	2.5	69
90	Structure and magnetic properties of high coercive NdFeB films with a perpendicular anisotropy. Applied Physics Letters, 2003, 82, 1751-1753.	3.3	61

#	Article	IF	CITATIONS
91	Age Hardening of Ultrafine Grained Al-Ti-Cr Alloys Fabricated by Continuous Electron Beam Evaporation. Materials Transactions, 2003, 44, 1955-1961.	1.2	1
92	Microstructure of Rapidly Solidified High Strength Al ₉₄ V ₄ Fe ₂ Alloy. Materials Transactions, 2003, 44, 1993-1998.	1.2	4
93	Magnetic properties and microstructures of \hat{I} ±-Fe/Nd[sub 2]Fe[sub 14]B nanocomposite microalloyed with Zr. Journal of Applied Physics, 2002, 91, 8174.	2.5	34
94	Local chemistry of a nanocrystalline high-strength Mg 97 Y 2 Zn 1 alloy. Philosophical Magazine Letters, 2002, 82, 543-551.	1.2	126
95	3次åfã,¢ãf^ãfãf—ãfãf¼ãf—ã«ã,`ã,<ãfŠãfŽçµœ™¶ç£œ€§æœ—™ã®è§£æž• Materia Japan, 2002, 41, 880-882	l0.1	0
96	Microstructure Feature of Bulk Glassy Cu ₆₀ Zr ₃₀ Ti ₁₀ Alloy in As-cast and Annealed States. Materials Transactions, 2002, 43, 2647-2650.	1.2	37
97	Nanocrystallization of Pd74Si18Au8 metallic glass. Intermetallics, 2002, 10, 1053-1060.	3.9	10
98	Microstructure and magnetic properties of microalloyed α-Fe/Nd2Fe14B nanocomposites. Journal of Magnetism and Magnetic Materials, 2002, 239, 437-440.	2.3	20
99	Artificial modulation of magnetic structures on a monatomic layer scale in Co/Ru superlattices. Applied Physics Letters, 2001, 78, 1436-1438.	3.3	37
100	Magnetic superlattices fabricated by monoatomic layer control. Surface Science, 2001, 493, 713-720.	1.9	6
101	Solid state amorphization in cold drawn Cu/Nb wires. Acta Materialia, 2001, 49, 389-394.	7.9	139
102	Nanoquasicrystalline phase formation in binary Zr–Pd and Zr–Pt alloys. Acta Materialia, 2001, 49, 3453-3462.	7.9	62
103	In situ observation of G. P. zones in an Al-Zn-Mg alloy under irradiation of electron beam. Journal of Materials Science Letters, 2001, 20, 1413-1414.	0.5	4
104	Microstructures of FePt–Al–O and FePt–Ag nanogranular thin films and their magnetic properties. Journal of Applied Physics, 2001, 90, 4708-4716.	2.5	99
105	Influence of oxygen on the crystallization behavior of Zr65Cu27.5Al7.5 and Zr66.7Cu33.3 metallic glasses. Acta Materialia, 2000, 48, 3985-3996.	7.9	165
106	Atom Probe Studies of Nanocrystallization of Amorphous Alloys. Materials Characterization, 2000, 44, 203-217.	4.4	43
107	Microstructural characterization of a rapidly solidified ultrahigh strength Al94.5Cr3Co1.5Ce1 alloy. Metallurgical and Materials Transactions A: Physical Metallurgy and Materials Science, 2000, 31, 607-614.	2.2	22
108	Microstructure and magnetic properties of FePt–Al–O granular thin films. Applied Physics Letters, 2000, 76, 3971-3973.	3.3	152

#	Article	IF	CITATIONS
109	Nanoquasicrystallization of binary Zr–Pd metallic glasses. Applied Physics Letters, 2000, 77, 1102-1104.	3.3	84
110	Direct evidence for oxygen stabilization of icosahedral phase during crystallization of Zr65Cu27.5Al7.5 metallic glass. Applied Physics Letters, 2000, 76, 55-57.	3.3	143
111	Microstructural characterization of an α-Fe/Nd2Fe14B nanocomposite magnet with a remaining amorphous phase. Journal of Applied Physics, 2000, 87, 8658-8665.	2.5	68
112	Microalloying effect of Cu and Nb on the microstructure and magnetic properties of Fe/sub 3/B/Nd/sub 2/Fe/sub 14/B nanocomposite permanent magnets. IEEE Transactions on Magnetics, 1999, 35, 3262-3264.	2.1	5
113	APFIM Studies of Nanocomposite Soft and Hard Magnetic Materials. Materials Science Forum, 1999, 307, 69-74.	0.3	7
114	Atom probe characterization of an α-Fe/Nd/sub 2/Fe/sub 14/B nanocomposite magnet with a remaining amorphous phase. IEEE Transactions on Magnetics, 1999, 35, 3295-3297.	2.1	8
115	Mechanism of grain size refinement of Fe3B/Nd2Fe14B nanocomposite permanent magnet by Cu addition. Journal of Applied Physics, 1999, 85, 2448-2450.	2.5	31
116	Impurity oxygen redistribution in a nanocrystallized Zr65Cr15Al10Pd10 metallic glass. Applied Physics Letters, 1999, 74, 812-814.	3.3	44
117	Microstructural evolution of Fe3B/Nd2Fe14B nanocomposite magnets microalloyed with Cu and Nb. Acta Materialia, 1999, 47, 4641-4651.	7.9	82
118	Cu clustering and Si partitioning in the early crystallization stage of an Fe73.5Si13.5B9Nb3Cu1 amorphous alloy. Acta Materialia, 1999, 47, 997-1006.	7.9	354
119	Effect of Cu On Microstructural Evolution of Nanocrystalline Soft and Hard Magnetic Materials. Materials Research Society Symposia Proceedings, 1999, 577, 507.	0.1	4
120	Effect of Cu Addition on the Microstructure and Magnetic Properties of an Fe3B/Nd2Fe14B Nanocomposite Magnet Journal of the Magnetics Society of Japan, 1999, 23, 1101-1104.	0.4	4
121	Precipitations in an Yttrium-Containing Low-Expansion Superalloy. Journal of Materials Science, 1998, 33, 5069-5077.	3.7	7
122	Partitioning of Ga and Co atoms in a Fe3B/Nd2Fe14B nanocomposite magnet. Journal of Applied Physics, 1998, 83, 7769-7775.	2.5	64
123	Oxidation Behavior of a Ni â€â€‰La2 O 3 Codeposited Film on Nickel. Journal of the Electrochemic 1998, 145, 389-398.	al Society	, 64
124	Apfim and HREM Studies of Nanocomposite Soft and Hard Magnetic Materials. Microscopy and Microanalysis, 1998, 4, 108-109.	0.4	0
125	Microstructural Characterization of Rapidly Solidified Ultrahigh Strength Aluminum Alloys. Microscopy and Microanalysis, 1998, 4, 98-99.	0.4	0
126	Characterization of nanocrystalline Ni33Zr67alloy. Journal of Applied Physics, 1997, 81, 1103-1108.	2.5	15

#	Article	IF	CITATIONS
127	Title is missing!. Journal of Materials Science, 1997, 32, 2501-2507.	3.7	3
128	Microstructure of second-phase particles in Ti-5Al-4Sn-2Zr-1Mo-0.25Si-1Nd alloy. Metallurgical and Materials Transactions A: Physical Metallurgy and Materials Science, 1997, 28, 1595-1605.	2.2	18
129	Microstructural characterization of nanocrystalline materials. Journal of Materials Science Letters, 1995, 14, 1536-1540.	0.5	35
130	High-resolution transmission-electron-microscopy observation of the ultra-fine structure of natural magnetite. Journal of Applied Crystallography, 1994, 27, 96-102.	4.5	4
131	Structure and property of polycrystalline (Fe0.99Mo0.01)78Si9B13alloys. Journal of Applied Physics, 1993, 74, 4501-4505.	2.5	12
132	Snoek Relaxation in bcc Metals and High Damping β-Ti Alloys. Materials Science Forum, 0, 614, 175-180.	0.3	9
133	Variation of the Reversed Austenite Amount with the Tempering Temperature in a Fe-13%Cr-4%Ni-Mo	0.3	6